

OPERATION OF A HOMEOSTATIC SLEEP SWITCH

Diogo Pimentel^{1*}, Jeffrey M. Donlea^{1*}, Clifford B. Talbot¹, Seoho M. Song¹, Alexander J. F. Thurston¹, and Gero Miesenböck¹

¹ Centre for Neural Circuits and Behaviour, University of Oxford, Tinsley Building,
Mansfield Road, Oxford, OX1 3SR, United Kingdom

* These authors contributed equally to this work.

Sleep disconnects animals from the external world, at considerable risks and costs that must be offset by a vital benefit. Insight into this mysterious benefit will come from understanding sleep homeostasis: to monitor sleep need, an internal bookkeeper must track physiological changes that are linked to the core function of sleep¹. In *Drosophila*, a crucial component of the machinery for sleep homeostasis is a cluster of neurons innervating the dorsal fan-shaped body (dFB) of the central complex^{2,3}. Artificial activation of these cells induces sleep², whereas reductions in excitability cause insomnia^{3,4}. dFB neurons in sleep-deprived flies tend to be electrically active, with high input resistances and long membrane time constants, while neurons in rested flies tend to be electrically silent³. Correlative evidence thus supports the simple view that homeostatic sleep control works by switching sleep-promoting neurons between active and quiescent states³. Here we demonstrate state switching by dFB neurons, identify dopamine as a neuromodulator that operates the switch, and delineate the switching mechanism. Arousing dopamine⁴⁻⁸ caused transient hyperpolarization of dFB neurons within tens of milliseconds and lasting excitability suppression within minutes. Both effects were transduced by Dop1R2 receptors and mediated by potassium conductances. The switch to electrical silence involved the downregulation of voltage-gated A-type currents carried by Shaker and Shab and the upregulation of voltage-independent leak currents through a two-pore domain potassium channel we term Sandman. Sandman is encoded by the *CG8713* gene and translocates to the plasma membrane in response to dopamine. dFB-restricted interference with the expression of Shaker or Sandman decreased or increased sleep, respectively, by slowing the repetitive discharge of dFB neurons in the ON state or blocking their entry into the OFF state. Biophysical changes in a small population of neurons are thus linked to the control of sleep-wake state.

We recorded from dFB neurons (which were marked by *R23E10-GAL4* or *R23E10-LexA* driven GFP expression³) while head-fixed flies walked or rested on a spherical treadmill. Because inactivity is a necessary correlate but insufficient proof of sleep, we restricted our analysis to awakening, which we defined as a locomotor bout following ≥ 5 minutes of rest^{9,10}, during which the recorded dFB neuron had been persistently spiking. To deliver wake-promoting signals, we expressed the optogenetic actuator^{5,11} CsChrimson under *TH-GAL4* control in the majority of dopaminergic neurons, including the PPL1 and PPM3 clusters¹², whose FB-projecting members have been implicated in sleep control^{4,8}. Illumination at 630 nm, sustained for 1.5 s to release a bolus of dopamine (Extended Data

Fig. 1), effectively stimulated locomotion (32/38 trials; Fig. 1a, b). dFB neurons paused in successful (but not in unsuccessful) trials (Fig. 1a, b), and their membrane potentials dipped by 2–13 mV (7.50 ± 0.56 mV; mean \pm s.e.m.) below the baseline during tonic activity (Fig. 1a, c). When flies bearing an undriven *CsChrimson* transgene were photostimulated, neither physiological nor behavioural changes were apparent (Fig. 1d–f). The tight correlation between the suppression of dFB neuron spiking and the initiation of movement ($P < 0.0001$, Fisher's exact test) might, however, merely mirror a causal dopamine effect elsewhere, as *TH-GAL4* labels dopaminergic neurons throughout the brain¹². Because localized dopamine applications to dFB neuron dendrites similarly caused awakening (Fig. 3d, below), we consider this possibility remote.

Flies with enhanced dopaminergic transmission exhibit a short-sleeping phenotype that requires the presence of a D1-like receptor in dFB neurons^{4,8}, suggesting that dopamine acts directly on these cells. dFB-restricted RNA-mediated interference (RNAi) confirmed this notion and pinpointed Dop1R2 as the responsible receptor (Fig. 2a), a conclusion reinforced by analysis of the mutant *Dop1R2*^{M108664} allele (Extended Data Fig. 2a–c). Prior evidence that Dop1R1, a receptor not involved in regulating baseline sleep⁸, confers responsiveness to dopamine when expressed in the dFB^{4,8} indicates that either D1-like receptor can fulfill the role normally played by Dop1R2. Loss of Dop1R2 increased sleep during the day and the late hours of the night, by prolonging sleep bouts without affecting their frequency (Extended Data Fig. 2a, d, e). This sleep pattern is consistent with reduced sensitivity to a dopaminergic arousal signal.

To confirm the identity of the effective transmitter, avoid dopamine release outside the dFB, and reduce the transgene load for subsequent experiments, we replaced optogenetic manipulations of the dopaminergic system with pressure ejections of dopamine onto dFB neuron dendrites (Fig. 2b). Like optogenetically stimulated secretion, focal application of dopamine hyperpolarized the cells and suppressed their spiking (Fig. 2c, Extended Data Fig. 3a, b). The inhibitory responses could be blocked at several nodes of an intracellular signaling pathway that connects the activation of dopamine receptors to the opening of potassium conductances (Fig. 2c, Extended Data Fig. 3b): by RNAi-mediated knockdown of Dop1R2; by the inclusion in the patch pipette of pertussis toxin (PTX), which inactivates heterotrimeric G-proteins of the $G_{i/o}$ family¹³; and by replacing intracellular potassium with caesium, which obstructs the pores of G-protein-coupled inward-rectifier channels¹⁴.

Elevating the chloride reversal potential above resting potential left the polarity of the responses unchanged (Fig. 2c, Extended Data Fig. 3b), corroborating that potassium conductances mediate the bulk of dopaminergic inhibition.

Coupling of Dop1R2 to $G_{i/o}$, though documented in a heterologous system¹⁵, represents a sufficiently unusual transduction mechanism for a predicted D1-like receptor to prompt us to verify its significance. Like the loss of Dop1R2, temperature-inducible expression of PTX in dFB neurons increased overall sleep time by extending sleep bout length (Extended Data Fig. 2f, g).

While a single pulse of dopamine transiently hyperpolarized dFB neurons and inhibited their spiking, prolonged dopamine applications (50 ms pulses at 10 Hz, or 20 Hz optogenetic stimulation, both sustained for 2–10 min) switched the cells from electrical excitability (ON) to quiescence (OFF) (Fig. 3a–c, Extended Data Fig. 4a–c). The switching process required dopamine as well as Dop1R2 (Fig. 3b, c), but once the switch had been actuated the cells remained in the OFF state—and flies, awake (Fig. 3d)—without a steady supply of transmitter. Input resistances and membrane time constants dropped to 53.3 ± 1.8 and $24.0 \pm 1.3\%$ of their initial values (means \pm s.e.m., $n=15$ cells; Fig. 3b,c), and depolarizing currents no longer elicited action potentials (15/15 cells) (Fig. 3a, Extended Data Fig. 4a). The biophysical properties of single dFB neurons, recorded in the same individual before and after operating the dopamine switch, varied as widely as those in sleep-deprived and rested flies³.

Dopamine-induced changes in input resistance and membrane time constant occurred from similar baselines in all genotypes (Extended Data Fig. 5a, b) and followed single-exponential kinetics with time constants of 1.07–1.10 minutes (Fig. 3b, c). The speed of conversion points to posttranslational modification and/or translocation of ion channels between intracellular pools and the plasma membrane as the underlying mechanism(s). In 7/15 cases, we held recordings long enough to observe the spontaneous recommencement of spiking (Fig. 3a, d), which was accompanied by a rise to baseline of input resistance and membrane time constant, after 7–60 minutes of quiescence (mean \pm s.e.m = 25.86 ± 7.61 minutes). The temporary suspension of electrical output is thus part of the normal activity cycle of dFB neurons and not a dead end brought on by our experimental conditions.

dFB neurons in the ON state expressed two types of potassium current: voltage-dependent A-type¹⁶ and voltage-independent non-A-type currents (Fig. 3e–g, Extended Data Fig. 6a–c). The current-voltage (I-V) relation of I_A resembled that of Shaker, the prototypical A-type channel^{17,18}: no current flowed below -50 mV, the approximate voltage threshold of Shaker^{17,18}; above -40 mV, peak currents increased steeply with voltage (Fig. 3e, f) and inactivated with a time constant¹⁸ of 7.5 ± 2.1 ms (mean \pm s.e.m., $n=7$ cells; Extended Data Fig. 6c, d). Non-A-type currents showed weak outward rectification with a reversal potential of -80 mV (Fig. 3e, g), consistent with potassium as the permeant ion, and no inactivation (Extended Data Fig. 6b).

Switching the neurons OFF changed both types of potassium current. I_A diminished by one third (Fig. 3e, f), whereas $I_{\text{non-A}}$ nearly quadrupled when quantified between resting potential and spike threshold (Fig. 3g). The weak rectification of $I_{\text{non-A}}$ in the ON state vanished in the OFF state, giving way to the linear I-V relationship of an ideal leak conductance (Fig. 3e, g). dFB neurons thus upregulate I_A in the sleep-promoting ON state (Fig. 3e, f). When dopamine switches the cells OFF, voltage-dependent currents are attenuated and leak currents augmented (Fig. 3e–g). This see-saw form of regulation should be sensitive to perturbations of the neurons' ion channel inventory: depletion of voltage-gated A-type (K_V) channels (which predominate in the ON state) should tip the cells toward the OFF state; conversely, loss of leak channels (which predominate in the OFF state) should favour the ON state. To test these predictions, we examined sleep in flies carrying *R23E10-GAL4* driven RNAi transgenes for dFB-restricted interference with individual potassium channels.

RNAi-mediated knockdown of two of the five K_V channel types of *Drosophila*¹⁹ (Shaker and Shab) reduced sleep relative to parental controls, while knockdown of the remaining three types had no effect (Fig. 4a). Biasing the potassium channel repertoire of dFB neurons against A-type conductances thus tilts the neurons' excitable state toward quiescence (Fig. 4b–f), causing insomnia (Fig. 4a), but leaves transient and sustained dopamine responses unaffected (Fig. 4e–g, Extended Data Fig. 3b). The seemingly counterintuitive conclusion that reducing a potassium current would decrease, not increase, action potential discharge is explained by a requirement for A-type channels in generating repetitive activity^{16,20} of the kind displayed by dFB neurons during sleep (Fig. 1). Depleting Shaker from dFB neurons shifted the interspike interval distribution toward longer values (Fig. 4d), as would be expected if K_V channels with slow inactivation kinetics replaced rapidly inactivating Shaker

as the principal force opposing the generation of the next spike. These findings identify a potential mechanism for the short-sleeping phenotypes caused by mutations in *shaker*²¹, its β subunit *hyperkinetic*²², or its regulator *sleepless*²³ (Extended Data Fig. 7).

Leak conductances are typically formed by two-pore domain potassium (K_{2P}) channels²⁴. dFB-restricted RNAi of one member of the 11-strong family of *Drosophila* K_{2P} channels¹⁹, encoded by the *CG8713* gene, increased sleep relative to parental controls; interference with the remaining 10 K_{2P} channels had no effect (Fig. 4a). Recordings from dFB neurons after knock-down of the *CG8713* gene product, which we term Sandman, revealed undiminished non-A-type currents in the ON state (Fig. 4c) and intact responses to a single pulse of dopamine (Fig. 4g, Extended Data Fig. 3b) but a defective OFF switch: during prolonged dopamine applications, $I_{\text{non-A}}$ failed to rise (Fig. 4c), input resistances and membrane time constants remained at their elevated levels (Fig. 4b, e, f, Extended Data Fig. 5), and the neurons continued to fire action potentials (7/7 cells) (Fig. 4b). Blocking vesicle exocytosis in the recorded cell with botulinum neurotoxin C (BoNT/C)²⁵ similarly disabled the OFF switch (Fig. 4c, e, f). This, combined with the absence of detectable Sandman currents in the ON state (Fig. 4c), suggests that Sandman is internalized in electrically active cells and recycled to the plasma membrane when dopamine switches the neurons OFF.

Because dFB neurons lacking Sandman spike persistently even after prolonged dopamine exposure (Fig. 4b), voltage-gated sodium channels remain functional in the OFF state. The difficulty of driving control cells to action potential threshold in this state (Fig. 3a, Extended Data Fig. 4a) must therefore be due to a lengthening of electrotonic distance between sites of current injection and spike generation. This lengthening is an expected consequence of a current leak, which may uncouple the axonal spike generator from somatodendritic synaptic inputs or pacemaker currents when sleep need is low.

The two kinetically and mechanistically distinct actions of dopamine on dFB neurons— instant, but transient, hyperpolarization and a delayed, but lasting, switch in excitable state— ensure that transitions to vigilance can be both immediate and sustained, providing speedy alarm responses and stable homeostatic control. The key to stability lies in the switching behaviour of dFB neurons, which is driven by dopaminergic input accumulated over time. Unlike bistable neurons²⁶⁻²⁸, in which two activity regimes coexist for the same set of conductances, dFB neurons switch regimes only when their membrane current densities

change. Our analysis of how dopamine effects such a change, from activity to silence, has uncovered elements familiar from other modulated systems^{20,27-30}: simultaneous, antagonistic regulation of multiple conductances^{20,29}; reduction of I_A (ref. 20); and modulation of leak currents²⁴. We currently know little about the reverse transition, from silence to activity, except that mutating the Rho-GTPase-activating protein Crossveinless-c locks dFB neurons in the OFF state, resulting in severe insomnia and an inability to correct sleep deficits³. Discovering the signals and processes that switch sleep-promoting neurons back ON will hold important clues to the vital function of sleep.

1. Saper, C. B., Fuller, P. M., Pedersen, N. P., Lu, J. & Scammell, T. E. Sleep state switching. *Neuron* **68**, 1023–1042 (2010).
2. Donlea, J. M., Thimman, M. S., Suzuki, Y., Gottschalk, L. & Shaw, P. J. Inducing sleep by remote control facilitates memory consolidation in *Drosophila*. *Science* **332**, 1571–1576 (2011).
3. Donlea, J. M., Pimentel, D. & Miesenböck, G. Neuronal machinery of sleep homeostasis in *Drosophila*. *Neuron* **81**, 860–872 (2014).
4. Liu, Q., Liu, S., Kodama, L., Driscoll, M. R. & Wu, M. N. Two dopaminergic neurons signal to the dorsal fan-shaped body to promote wakefulness in *Drosophila*. *Curr Biol* **22**, 2114–2123 (2012).
5. Lima, S. Q. & Miesenböck, G. Remote control of behavior through genetically targeted photostimulation of neurons. *Cell* **121**, 141–152 (2005).
6. Andretic, R., van Swinderen, B. & Greenspan, R. J. Dopaminergic modulation of arousal in *Drosophila*. *Curr Biol* **15**, 1165–1175 (2005).
7. Kume, K., Kume, S., Park, S. K., Hirsh, J. & Jackson, F. R. Dopamine is a regulator of arousal in the fruit fly. *J Neurosci* **25**, 7377–7384 (2005).
8. Ueno, T. *et al.* Identification of a dopamine pathway that regulates sleep and arousal in *Drosophila*. *Nat Neurosci* **15**, 1516–1523 (2012).
9. Shaw, P. J., Cirelli, C., Greenspan, R. J. & Tononi, G. Correlates of sleep and waking in *Drosophila melanogaster*. *Science* **287**, 1834–1837 (2000).
10. Hendricks, J. C. *et al.* Rest in *Drosophila* is a sleep-like state. *Neuron* **25**, 129–138 (2000).
11. Zemelman, B. V., Lee, G. A., Ng, M. & Miesenböck, G. Selective photostimulation of genetically chARGed neurons. *Neuron* **33**, 15–22. (2002).
12. Claridge-Chang, A. *et al.* Writing memories with light-addressable reinforcement circuitry. *Cell* **139**, 405–415 (2009).
13. Bokoch, G. M., Katada, T., Northup, J. K., Ui, M. & Gilman, A. G. Purification and properties of the inhibitory guanine nucleotide-binding regulatory component of adenylate cyclase. *J. Biol. Chem.* **259**, 3560–3567 (1984).
14. Andrade, R. & Nicoll, R. A. Pharmacologically distinct actions of serotonin on single pyramidal neurones of the rat hippocampus recorded in vitro. *J Physiol (Lond)* **394**, 99–124 (1987).
15. Reale, V., Hannan, F., Hall, L. M. & Evans, P. D. Agonist-specific coupling of a cloned *Drosophila melanogaster* D1-like dopamine receptor to multiple second messenger pathways by synthetic agonists. *J Neurosci* **17**, 6545–6553 (1997).

16. Connor, J. A. & Stevens, C. F. Prediction of repetitive firing behaviour from voltage clamp data on an isolated neurone soma. *J Physiol (Lond)* **213**, 31–53 (1971).
17. Timpe, L. C. *et al.* Expression of functional potassium channels from Shaker cDNA in *Xenopus* oocytes. *Nature* **331**, 143–145 (1988).
18. Iverson, L. E., Tanouye, M. A., Lester, H. A., Davidson, N. & Rudy, B. A-type potassium channels expressed from Shaker locus cDNA. *Proc Natl Acad Sci USA* **85**, 5723–5727 (1988).
19. Littleton, J. T. & Ganetzky, B. Ion channels and synaptic organization: analysis of the *Drosophila* genome. *Neuron* **26**, 35–43 (2000).
20. Harris-Warrick, R. M., Coniglio, L. M., Barazangi, N., Guckenheimer, J. & Gueron, S. Dopamine modulation of transient potassium current evokes phase shifts in a central pattern generator network. *J Neurosci* **15**, 342–358 (1995).
21. Cirelli, C. *et al.* Reduced sleep in *Drosophila* Shaker mutants. *Nature* **434**, 1087–1092 (2005).
22. Bushey, D., Huber, R., Tononi, G. & Cirelli, C. *Drosophila* Hyperkinetic mutants have reduced sleep and impaired memory. *J Neurosci* **27**, 5384–5393 (2007).
23. Koh, K. *et al.* Identification of SLEEPLESS, a sleep-promoting factor. *Science* **321**, 372–376 (2008).
24. Enyedi, P. & Czirják, G. Molecular background of leak K⁺ currents: two-pore domain potassium channels. *Physiol Rev* **90**, 559–605 (2010).
25. Schiavo, G., Matteoli, M. & Montecucco, C. Neurotoxins affecting neuroexocytosis. *Physiol Rev* **80**, 717–766 (2000).
26. Hounsgaard, J., Hultborn, H., Jespersen, B. & Kiehn, O. Bistability of alpha-motoneurons in the decerebrate cat and in the acute spinal cat after intravenous 5-hydroxytryptophan. *J Physiol (Lond)* **405**, 345–367 (1988).
27. Marder, E., Abbott, L. F., Turrigiano, G. G., Liu, Z. & Golowasch, J. Memory from the dynamics of intrinsic membrane currents. *Proc Natl Acad Sci USA* **93**, 13481–13486 (1996).
28. Marder, E. & Thirumalai, V. Cellular, synaptic and network effects of neuromodulation. *Neural Netw* **15**, 479–493 (2002).
29. Baxter, D. A. & Byrne, J. H. Serotonergic modulation of two potassium currents in the pleural sensory neurons of *Aplysia*. *J Neurophysiol* **62**, 665–679 (1989).
30. Nicola, S. M., Surmeier, J. & Malenka, R. C. Dopaminergic modulation of neuronal excitability in the striatum and nucleus accumbens. *Annu Rev Neurosci* **23**, 185–215 (2000).

Methods

Drosophila strains and culture

Driver lines *R23E10-GAL4* or *R23E10-LexA*³¹ and *TH-GAL4*³² were used to target dFB neurons and dopaminergic neurons, respectively. Effector transgenes encoded fluorescent markers for visually guided patch-clamp recordings (*UAS-CD8::GFP*³³ and *lexAop-CD2::GFP*³⁴); a temperature-inducible system³⁵ for the expression of pertussis toxin³⁶ (*UAS-PTX*; *tubP-GAL80^{ts}*); the optogenetic actuator CsChrimson³⁷; and RNAi constructs³⁸, along with *UAS-Dcr2*, to interfere with the expression of the dopamine receptors Dop1R1 (107058KK), Dop1R2 (105324KK), DopR2 (11471GD), and DopEcR (103494KK); the K_v channels Shaker (104474KK), Shab (102218KK), Shal (103363KK), Shaw (110589KK), and Shaw1 (100980KK); the interacting partners of Shaker, Hyperkinetic (101402KK) and Sleepless (104533KK); and the K_{2P} channels Task7 (8565GD), Task6 (9073GD), Ork1 (104883KK), CG1688 (30270GD), CG10864 (8302GD), CG34396 (100436KK), CG43155 (101483KK), CG42594 (46415GD), CG8713 (47977GD), CG9194 (110628KK), and CG42340 (104521KK). Codes in parentheses identify transformants in the GD and KK libraries of the Vienna *Drosophila* Resource Center. The genotype of control flies in electrophysiological experiments was *w¹¹¹⁸*; *UAS-CD8::GFP*; *R23E10-GAL4*.

Fly stocks were grown on media of sucrose, yeast, molasses, and agar under a 12 h light : 12h dark cycle at 25 °C unless they expressed GAL80^{ts}; in this case the experimental animals and all relevant controls were grown at 18°C. Flies expressing CsChrimson were transferred to food supplemented with 2 mM all-trans retinal upon eclosion. All studies were performed on animals aged 3–10 days. Flies were routinely sleep-deprived³⁹ for >12 h before electrophysiological recordings to increase the likelihood of finding dFB neurons in the electrically active ON state after break-in.

Movement tracking, electrophysiology, and optogenetics

Male and female flies with a dorsal cranial window were head-fixed to a custom mount, using thermoplastic wax with a melting point of 52 °C (Agar Scientific), and placed on a spherical treadmill^{40,41}. The treadmill consisted of an air-supported trackball made of extruded styrofoam (13 mm diameter; 50 mg) in a 14 mm tube. An image of a small region of the ball's surface under 640 nm LED illumination was relayed onto the sensor of an optical mouse (Logitech M-U0017). The sensor was interfaced with a microcontroller board (Arduino

Due) based on the Atmel SAM3X CPU and read out in real time using the onboard D/A converter. The resolution of the readout corresponds to 4 mm/s increments in the tangential speed of the trackball.

The brain was continuously superfused with extracellular solution equilibrated with 95% O₂-5% CO₂ and containing 103 mM NaCl, 3 mM KCl, 5 mM TES, 8 mM trehalose, 10 mM glucose, 7 mM sucrose, 26 mM NaHCO₃, 1 mM NaH₂PO₄, 1.5 mM CaCl₂, 4 mM MgCl₂, pH 7.3. Somata of GFP-labeled dFB neurons were visually targeted with borosilicate glass electrodes (7-13 M Ω). The internal solution contained 140 mM potassium aspartate, 10 mM HEPES, 1 mM KCl, 4 mM MgATP, 0.5 mM Na₃GTP, 1 mM EGTA, pH 7.3. Where indicated, 140 mM potassium aspartate was replaced with 140 mM KCl or 140 mM caesium aspartate, or the internal solution was supplemented with 2 μ g/ml pertussis toxin (Tocris) or 1.5 μ g/ml botulinum neurotoxin C light chain (List Biological Laboratories). Neurons were dialyzed with toxin-containing internal solutions for 10–15 min before measurements.

Signals were acquired with a Multiclamp 700B amplifier (Molecular Devices), filtered at 6–10 kHz, and digitized at 10–20 kHz using an ITC-18 data acquisition board (InstruTECH) controlled by the Nclamp/Neuromatic package. Data were analyzed using Neuromatic software (www.neuromatic.thinkrandom.com) and custom procedures in Igor Pro (Wavemetrics) and MATLAB (The MathWorks).

Voltage-clamp experiments were performed in the presence of 1 μ M tetrodotoxin (Tocris) and 200 nM cadmium to block sodium and calcium channels, respectively. Neurons were taken in 10 mV increments from holding potentials of –110 or –30 mV to test potentials between –100 and 40 mV (Extended Data Fig. 6a, b). When the cells were held at –110 mV, depolarization steps (1 s duration) elicited the full complement of potassium currents; when the cells were held at –30 mV, voltage-gated channels inactivated and the evoked potassium currents lacked the I_A (A-type or fast outward) component⁴². The non A-type component was quantified at the steady state (end) of the current response. Digital subtraction of the non-A-type component from the full complement of potassium currents (that is, the currents evoked from a hyperpolarized holding potential of –110 mV) gave an estimate of I_A (Extended Data Fig. 6c), which was taken to be the difference between the peak current and any residual steady state current in the difference trace.

Interspike intervals were determined from voltage responses to a standard series of depolarizing current steps (5 pA increments from 0 to 150 pA, 1 s duration). Spikes were detected by finding minima in the second derivative of the membrane potential trace. Interspike intervals at all levels of injected current were pooled for the calculation of frequency distributions.

For photostimulation of CsChrimson-expressing neurons³⁷, a 630 nm LED (Multicomp OSW-4388) was focused onto the head of the fly with a 60 mm lens (Thorlabs) and controlled by a TTL-triggered dimmable constant current LED driver (Recom RCD-24-0.70/W/X3). Optical power at the sample was $\sim 28 \text{ mW/cm}^2$. To induce state switching, light was delivered in a pulsatile fashion in 5 s cycles. The first 3.5 s of each cycle consisted of 20 Hz trains of 3 ms optical pulses. Illumination was paused during the remaining 1.5 s of each cycle, and a hyperpolarizing current pulse (-10 pA ; 1s) was applied to determine the membrane resistance and time constant.

For pharmacological applications of dopamine, patch pipettes were filled with 10 mM dopamine in extracellular solution and positioned in the centre of the GFP-labeled dendritic tuft of dFB neurons. To elicit transient dopamine responses, pressure (68 kPa) was applied in 250 ms pulses (Picospritzer III), resulting in the ejection of $\sim 40 \text{ pl}$ of solution. To induce state switching, dopamine was delivered in a pulsatile fashion in 5 s cycles. The first 3.5 s of each cycle consisted of 10 Hz trains of 50 ms pressure pulses. Dopamine delivery was paused during the remaining 1.5 s of each cycle, and a hyperpolarizing current pulse (-10 pA ; 1s) was applied to determine the membrane resistance and time constant.

Sleep measurements

Female flies were individually inserted into 65 mm glass tubes, loaded into the Trikinetics *Drosophila* Activity Monitor system, and housed under 12 h light : 12h dark conditions. Periods of inactivity (no beam breaks) lasting at least 5 minutes were classified as sleep^{9,10}. Immobile flies (< 2 beam breaks per 24 h) were excluded from analysis. Group sizes for sleep measurements (typically $n=16$ flies; in some cases multiples of 16) reflect the capacity of the Trikinetics *Drosophila* Activity Monitors, which were designed to accommodate 16 experimental flies along with 16 controls.

Statistics

Data were analyzed in Prism 6 (GraphPad). Group means were compared by one-way or two-way ANOVA, using repeated measures designs where appropriate, followed by planned pairwise post hoc analyses using Holm-Šidák's multiple comparisons test. Where the assumptions of normality or sphericity were violated (as indicated by Shapiro-Wilk and Brown-Forsythe tests, respectively), group means were compared by two-sided Mann-Whitney or Kruskal-Wallis tests, the latter followed by Dunn's multiple comparisons test. Contingencies between the suppression of dFB neuron activity and awakening were analyzed by Fisher's exact test. Interspike interval distributions were evaluated by Kolmogorov-Smirnov test, using the Bonferroni correction to adjust the level of statistical significance. No statistical methods were used to predetermine sample sizes.

31. Jenett, A. *et al.* A GAL4-driver line resource for Drosophila neurobiology. *Cell Rep* **2**, 991–1001 (2012).
32. Friggi-Grelin, F. *et al.* Targeted gene expression in Drosophila dopaminergic cells using regulatory sequences from tyrosine hydroxylase. *J Neurobiol* **54**, 618–627 (2003).
33. Lee, T. & Luo, L. Mosaic analysis with a repressible cell marker for studies of gene function in neuronal morphogenesis. *Neuron* **22**, 451–461 (1999).
34. Pfeiffer, B. D. *et al.* Refinement of tools for targeted gene expression in Drosophila. *Genetics* **186**, 735–755 (2010).
35. McGuire, S. E., Le, P. T., Osborn, A. J., Matsumoto, K. & Davis, R. L. Spatiotemporal rescue of memory dysfunction in Drosophila. *Science* **302**, 1765–1768 (2003).
36. Ferris, J., Ge, H., Liu, L. & Roman, G. G(o) signaling is required for Drosophila associative learning. *Nat Neurosci* **9**, 1036–1040 (2006).
37. Klapoetke, N. C. *et al.* Independent optical excitation of distinct neural populations. *Nat Methods* **11**, 338–346 (2014).
38. Dietzl, G. *et al.* A genome-wide transgenic RNAi library for conditional gene inactivation in Drosophila. *Nature* **448**, 151–156 (2007).
39. Shaw, P. J., Tononi, G., Greenspan, R. J. & Robinson, D. F. Stress response genes protect against lethal effects of sleep deprivation in Drosophila. *Nature* **417**, 287–291 (2002).
40. Buchner, E. Elementary movement detectors in an insect visual-system. *Biol Cybern* **24**, 85–101 (1976).
41. Seelig, J. D. *et al.* Two-photon calcium imaging from head-fixed Drosophila during optomotor walking behavior. *Nat Methods* **7**, 535–540 (2010).
42. Connor, J. A. & Stevens, C. F. Voltage clamp studies of a transient outward membrane current in gastropod neural somata. *J Physiol (Lond)* **213**, 21–30 (1971).

Acknowledgments. We thank S. Birman, R. Davis, B. Dickson, V. Jayaraman, L. Luo, G. Roman, G. Rubin, the Bloomington Stock Center, and the Vienna *Drosophila* Resource Center for flies. This work was supported by grants (to G.M.) from the Wellcome Trust, the Gatsby Charitable Foundation, and the National Institutes of Health. J.M.D. was the recipient of a postdoctoral fellowship from the Human Frontier Science Program; S.M.S. is a Commonwealth Scholar.

Author Contributions. D.P, J.M.D., and G.M. designed the study and analyzed the results. All electrophysiological recordings were done by D.P.; J.M.D. performed molecular manipulations and behavioural analyses with the help of S.M.S. and A.J.F.T. C.B.T. developed instrumentation. G.M. wrote the paper.

Author Information. The authors declare no competing financial interests. Correspondence and requests for materials should be addressed to G.M. (gero.miesenboeck@cncb.ox.ac.uk).

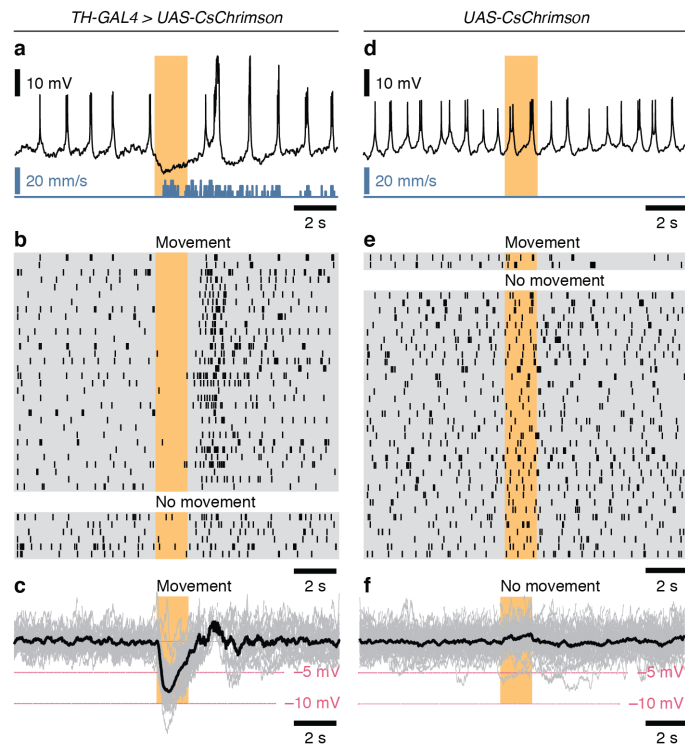


Figure 1. Optogenetic stimulation of dopaminergic neurons silences dFB neurons and promotes awakening. **a**, Membrane potential (black) of a dFB neuron and simultaneously recorded movement (blue) of a fly expressing CsChrimson in dopaminergic neurons. **b**, Spike rasters of dFB neurons in 38 trials. Photostimulation elicited a behavioural response in 32 trials (top) and no response in 6 trials (bottom). **c**, Individual (gray) and average (black) membrane potentials during the 32 trials with a behavioural response. Spikes are blanked for clarity. **d**, Membrane potential (black) of a dFB neuron and simultaneously recorded movement (blue) of a fly lacking CsChrimson expression in dopaminergic neurons. **e**, Spike rasters of dFB neurons in 59 trials. Photostimulation elicited a behavioural response in 2 trials (top) and no response in 57 trials; of these, 36 were randomly selected for display (bottom). **f**, Individual (gray) and average (black) membrane potentials during the 57 trials without a behavioural response. Spikes are blanked for clarity.

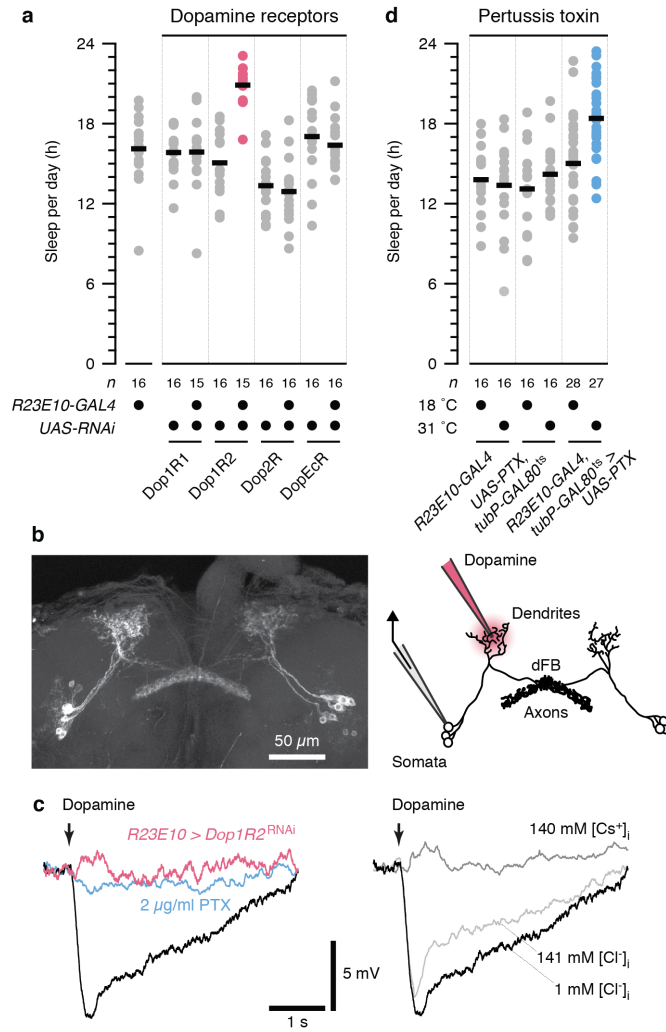


Figure 2. Dopamine inhibits dFB neurons via Dop1R2 and the transient opening of a potassium conductance. **a**, Sleep in flies expressing *R23E10-GAL4* driven RNAi targeting dopamine receptors and parental controls (circles denote individual flies; horizontal lines indicate group means). One-way ANOVA detected a significant genotype effect ($P < 0.0001$); red colour indicates a significant difference from both parental controls in pairwise post-hoc comparisons. **b**, *R23E10-GAL4* driven CD8::GFP expression in dFB neurons (left). Placement of pipettes for whole-cell recording and pharmacological stimulation (right). **c**, Membrane potentials of dFB neurons following a 250 ms pulse of dopamine, in control conditions of low intracellular chloride (1 mM; black, left and right); in cells expressing *R23E10-GAL4* driven RNAi targeting Dop1R2 (red, left); in the presence of 2 μ g/ml intracellular pertussis toxin (blue, left); in elevated intracellular chloride (141 mM; light gray, right); and in intracellular caesium (140 mM; dark gray, right). Traces are averages of 5 dopamine applications. **d**, Sleep in flies with temperature-inducible *R23E10-GAL4* driven expression of pertussis toxin and parental controls (circles denote individual flies; horizontal lines indicate group means). Two-way ANOVA detected a significant interaction between genotype and temperature ($P = 0.0143$); blue colour indicates a significant difference between inducing and non-inducing temperatures in pairwise post-hoc comparisons.

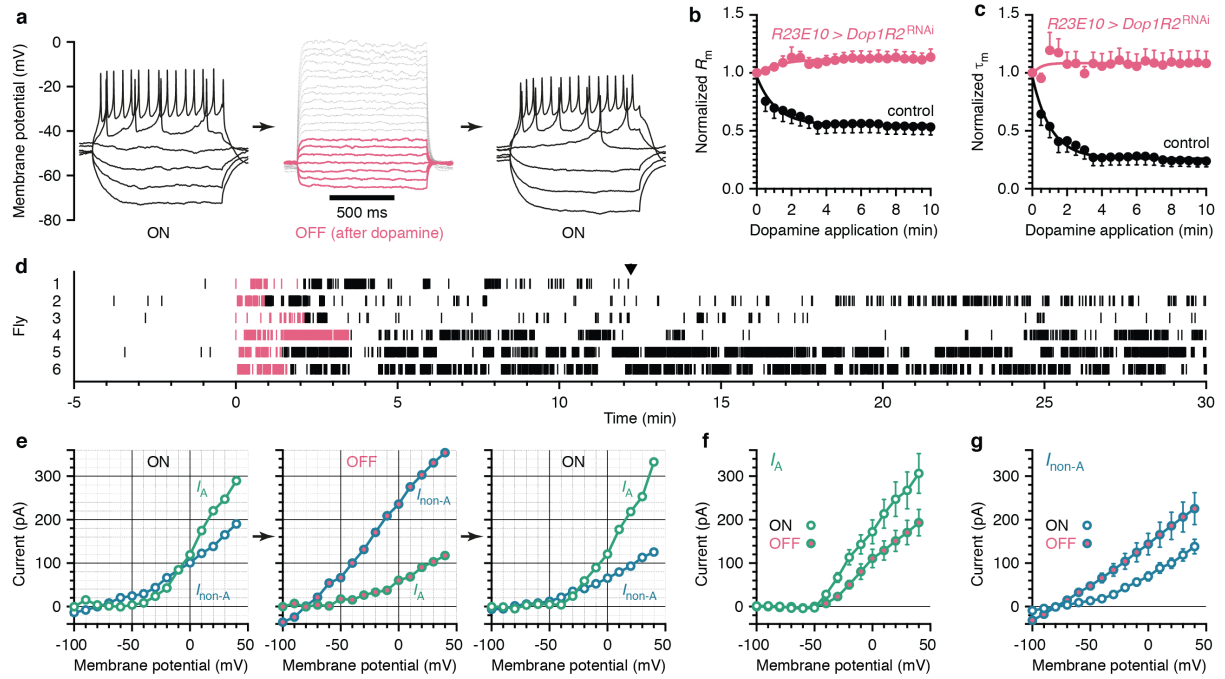


Figure 3. Dopamine switches dFB neurons to quiescence via rapid, reciprocal, and reversible modulation of voltage-dependent and -independent potassium conductances. **a**, A complete switching cycle in current clamp. Voltage responses to identical current steps were recorded in the same cell, before and after the application of dopamine. Red and gray traces in the OFF state (centre) indicate responses to current injections matching or exceeding those in the ON states, respectively. **b,c**, Time courses of changes in input resistance (R_m) and membrane time constant (τ_m) of dFB neurons during the application of dopamine, in controls (black, $n=15$ cells) and cells expressing *R23E10-GAL4* driven RNAi targeting Dop1R2 (red, $n=8$ cells). Data are means \pm s.e.m. Two-way repeated-measures ANOVA detected significant interactions between time and genotype ($P<0.0001$ for R_m ; $P<0.0001$ for τ_m). **d**, Movement rasters of 6 flies before, during, and after bilateral applications of dopamine to dFB neuron dendrites. Vertical marks denote rotations of the treadmill (surface velocity $> 4\text{mm/s}$, duration $> 50\text{ms}$). Red colour indicates the period of dopamine application, which started at 0 min (with the monitored dFB neuron in the ON state) and stopped when R_m fell to $\sim 60\%$ of its initial value. The arrowhead marks the spontaneous return to the ON state of the dFB neuron recorded in fly 1. Note the absence of movement thereafter. **e**, A complete switching cycle in voltage clamp. A-type (I_A , green) and non-A-type ($I_{\text{non-A}}$, blue) potassium currents evoked by identical voltage steps were recorded in the same cell, before and after the application of dopamine. **f**, Average ($n=7$ cells) current-voltage relationships of I_A in the ON state (white fills) and after dopamine-induced switching to the OFF state (red fills). Data are means \pm s.e.m. Two-way repeated-measures ANOVA detected a significant interaction between voltage and neuronal state ($P<0.0001$). **g**, Average ($n=7$ cells) current-voltage relationships of $I_{\text{non-A}}$ in the ON state (white fills) and after dopamine-induced switching to the OFF state (red fills). Data are means \pm s.e.m. Two-way repeated-measures ANOVA detected a significant interaction between voltage and neuronal state ($P<0.0001$).

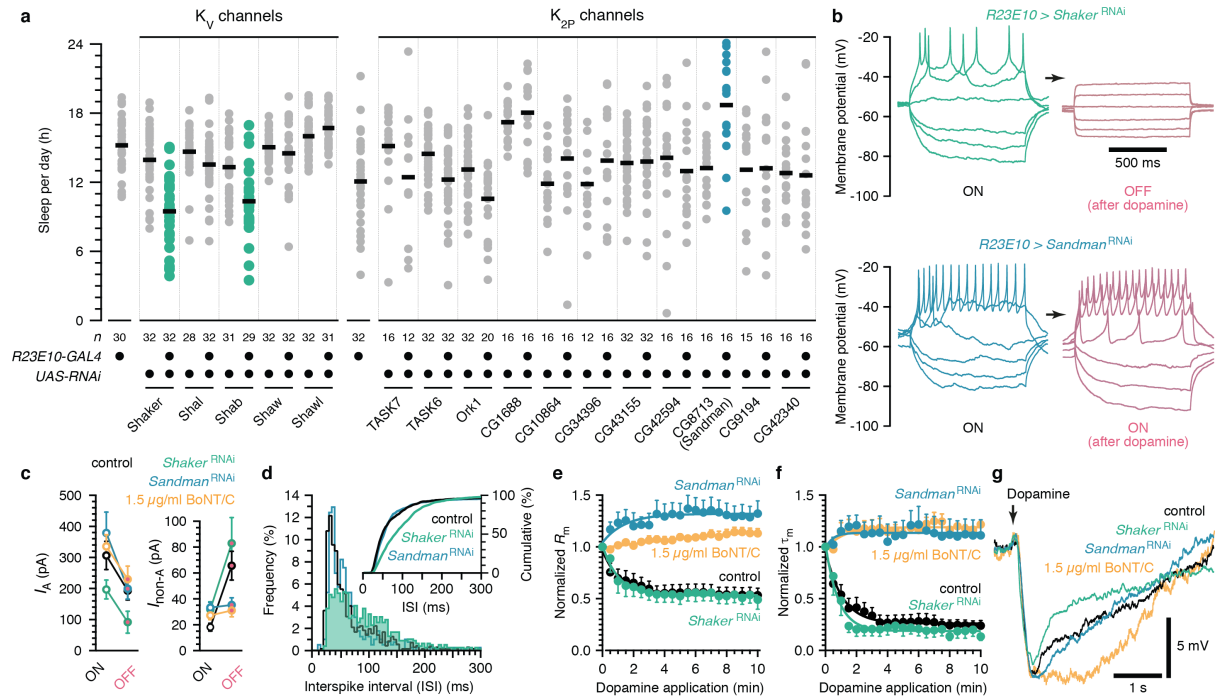
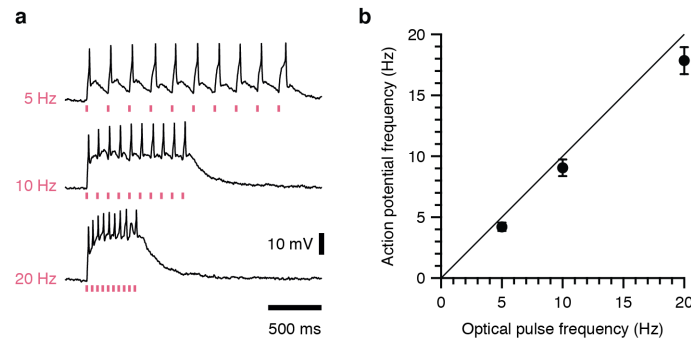
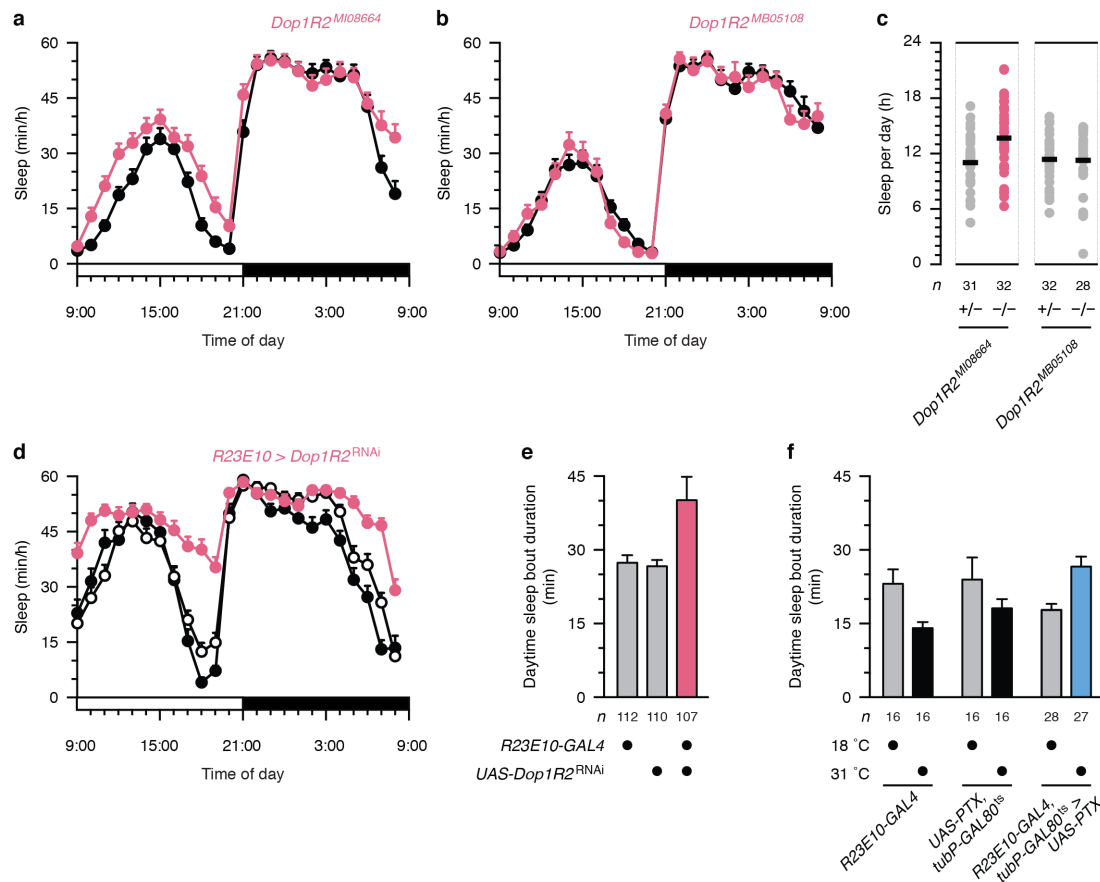


Figure 4. The targets of antagonistic modulation by dopamine—Shaker and Sandman—have opposing effects on sleep. **a**, Sleep in flies expressing $R23E10-GAL4$ driven RNAi targeting K_V or K_{2P} channels and parental controls (circles denote individual flies; horizontal lines indicate group means). One-way ANOVA detected significant genotype effects ($P < 0.0001$ for K_V channels; $P < 0.0001$ for K_{2P} channels); green and blue colours indicate significant differences from both parental controls in pairwise post-hoc comparisons. **b**, Examples of voltage responses of two dFB neurons to identical current steps, before and after the application of dopamine. The neurons expressed $R23E10-GAL4$ driven RNAi targeting Shaker (green, top) or Sandman (blue, bottom). **c**, Amplitudes of I_A at 40 mV (left) and I_{non-A} at -40 mV (right) in controls (black, $n=7$ cells), neurons expressing $R23E10-GAL4$ driven RNAi targeting Shaker (green, $n=7$ cells) or Sandman (blue, $n=8$ cells), and in the presence of 1.5 μ g/ml intracellular BoNT/C (orange, $n=8$ cells), in the ON state (white fills) and after dopamine-induced switching to the OFF state (red fills). Data are means \pm s.e.m. Two-way repeated-measures ANOVA detected significant effects of experimental condition ($P=0.0426$) and neuronal state ($P < 0.0001$) on I_A , and a significant interaction between experimental condition and neuronal state for I_{non-A} ($P=0.0018$). I_A was reduced in cells expressing $Shaker^{RNAi}$ relative to all other groups ($P=0.0409$). I_{non-A} differed between ON and OFF states in controls ($P=0.0005$) and cells expressing $Shaker^{RNAi}$ ($P=0.0003$), but not in cells expressing $Sandman^{RNAi}$ ($P=0.9119$) or containing BoNT/C ($P=0.9119$); I_{non-A} in the ON state did not differ among groups ($P=0.0782$). **d**, Frequency and cumulative frequency distributions (inset) of interspike intervals in controls (black) and neurons expressing $R23E10-GAL4$ driven RNAi targeting Shaker (green) or Sandman (blue). The interspike interval distribution of neurons expressing $Shaker^{RNAi}$ differed from that of the other groups ($P < 0.0001$ for both comparisons; Kolmogorov-Smirnov test). **e, f**, Time courses of changes in input resistance (R_m) and membrane time constant (τ_m) during the application of dopamine, in controls (black, $n=15$

cells), neurons expressing *R23E10-GAL4* driven RNAi targeting Shaker (green, $n=6$ cells) or Sandman (blue, $n=7$ cells), and in the presence of 1.5 $\mu\text{g/ml}$ intracellular BoNT/C (orange, $n=8$ cells). Data are means \pm s.e.m. Two-way repeated-measures ANOVA detected a significant interaction between time and experimental condition ($P<0.0001$ for R_m ; $P<0.0001$ for τ_m). dFB neurons expressing *Sandman*^{RNAi} or containing BoNT/C differed from controls ($P<0.0001$ for all pairwise comparisons), but flies expressing *Shaker*^{RNAi} did not ($P=0.9993$ for R_m ; $P=0.8743$ for τ_m). **g**, Membrane potentials of dFB neurons following a 250 ms pulse of dopamine, in control flies (black), flies expressing *R23E10-GAL4* driven RNAi targeting Shaker (green) or Sandman (blue), and in the presence of 1.5 $\mu\text{g/ml}$ intracellular BoNT/C (orange). Traces are averages of 5 dopamine applications.

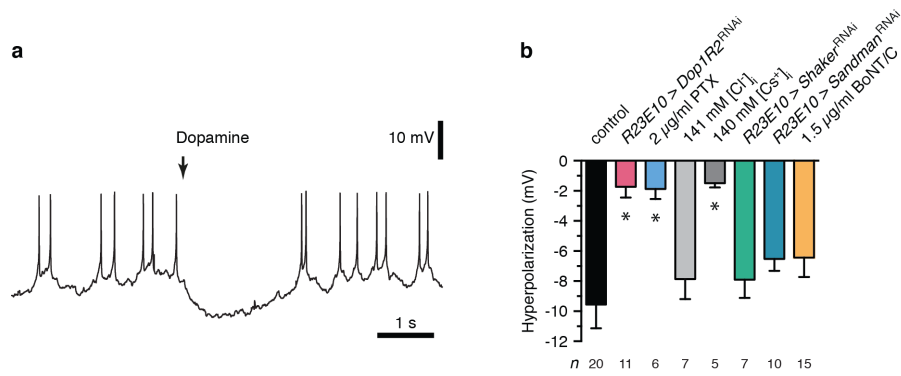


Extended Data Figure 1. Optogenetic stimulation of dopaminergic neurons. Dopaminergic neurons expressing CsChrimson under *TH-GAL4* control were driven with 3-ms pulses of 630-nm light at the indicated frequencies. Optical power at the sample was $\sim 28 \text{ mW/cm}^2$. **a**, Examples of voltage responses to optical pulse trains. **b**, The ratio of light-evoked action potentials to optical pulses was close to 1 at driving frequencies between 5 and 20 Hz ($n=36$ trials on 6 cells). Data are means \pm s.e.m.

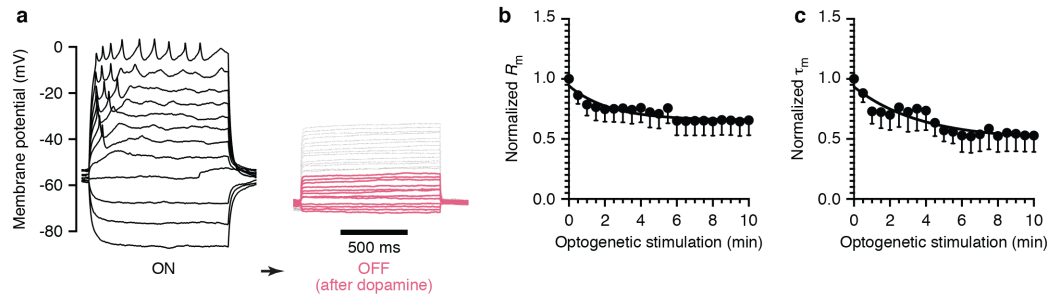


Extended Data Figure 2. Changes in sleep after interference with Dop1R2 signaling are consistent with diminished sensitivity to arousing dopamine. **a**, Sleep during a 24-hour day in homozygous carriers of the *Dop1R2*^{MI08664} allele (red, $n=32$ flies) and heterozygous controls (black, $n=31$ flies). Data are means \pm s.e.m. Two-way repeated-measures ANOVA detected a significant interaction between time of day and genotype ($P<0.0001$). **b**, Sleep during a 24-hour day in homozygous carriers of the *Dop1R2*^{MB05108} allele (red, $n=28$ flies) and heterozygous controls (black, $n=32$ flies). Data are means \pm s.e.m. Two-way repeated-measures ANOVA failed to detect a significant interaction between time of day and genotype ($P=0.4736$). **c**, Sleep in homozygous and heterozygous carriers of the *Dop1R2*^{MI08664} or *Dop1R2*^{MB05108} alleles (circles denote individual flies; horizontal lines indicate group means). Mann-Whitney tests detected a significant effect of the *Dop1R2*^{MI08664} allele ($P=0.0219$, red), but not of the *Dop1R2*^{MB05108} allele ($P=0.6750$). The *Dop1R2*^{MB05108} allele contains a transposon insertion in a non-coding region of the *Dop1R2* gene, which reduces mRNA levels in homozygous carriers by only 14% (ref. 4), thus explaining the lack of a phenotype. The inability of *Dop1R2*^{MB05108} to suppress the short-sleeping phenotype of flies with enhanced dopaminergic transmission⁴ does therefore not argue against a role of Dop1R2 in the dFB. **d**, Sleep during a 24-hour day in flies expressing *R23E10-GAL4* driven RNAi targeting Dop1R2 (red, $n=48$ flies) and parental controls (open symbols: *R23E10-GAL4*, $n=48$ flies; filled symbols: undriven *UAS-Dop1R2*^{RNAi}, $n=32$ flies). Data are means \pm s.e.m. Two-way repeated-measures ANOVA detected a significant interaction between time of day and genotype ($P<0.0001$). **e**, Average length of daytime sleep bouts in flies expressing *R23E10-GAL4* driven RNAi targeting Dop1R2 and parental

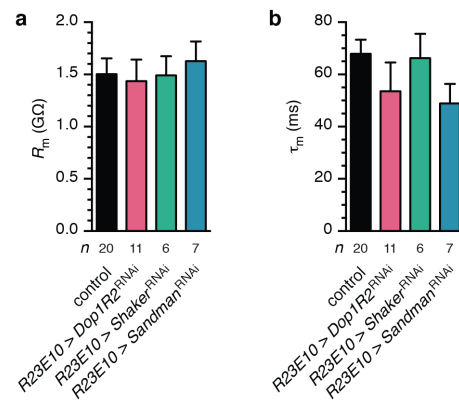
controls. Data are means \pm s.e.m. One-way ANOVA detected a significant genotype effect ($P=0.0015$); red colour indicates a significant difference from both parental controls in pairwise post-hoc comparisons. **f**, Average length of daytime sleep bouts in flies with temperature-inducible *R23E10-GAL4* driven expression of pertussis toxin and parental controls. Data are means \pm s.e.m. Two-way ANOVA detected a significant interaction between genotype and temperature ($P=0.0002$); blue colour indicates a significant increase upon switching from non-inducing to inducing temperatures in pairwise post-hoc comparisons.



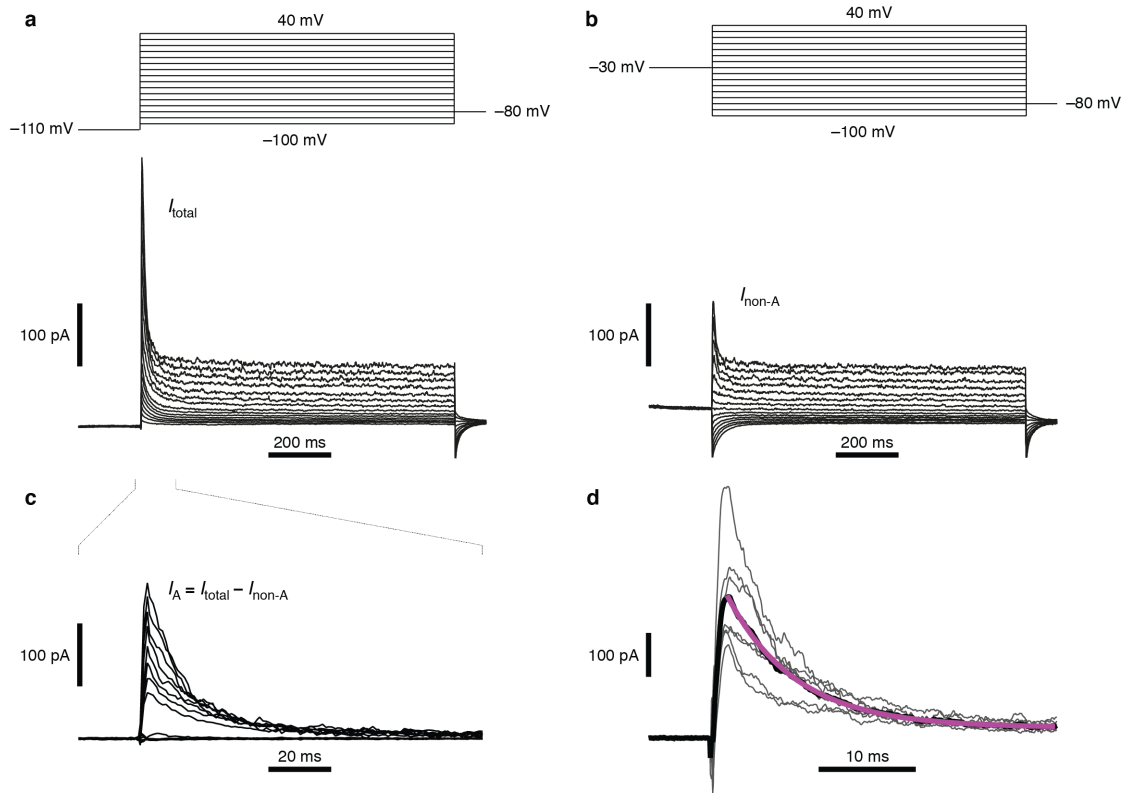
Extended Data Figure 3. Dopamine hyperpolarizes dFB neurons and inhibits their spiking. a, Membrane potential of a dFB neuron during a 250 ms pulse of dopamine. **b,** Average amplitude of hyperpolarization evoked by dopamine in the indicated numbers of cells. Data are means \pm s.e.m. Kruskal-Wallis test detected a significant difference between groups ($P < 0.0001$); asterisks indicate significant differences from control conditions in pairwise post-hoc comparisons.



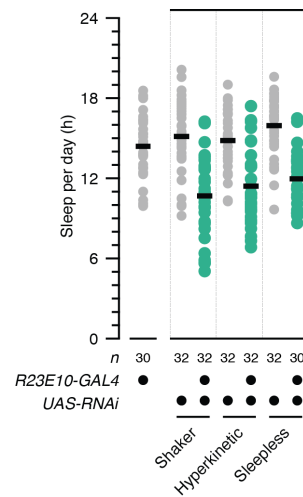
Extended Data Figure 4. Optogenetic stimulation of dopaminergic neurons switches dFB neurons to quiescence. Flies expressing CsChrimson under *TH-GAL4* control in dopaminergic neurons were photostimulated with 3 ms pulses of 630 nm light at 20 Hz. **a**, Voltage responses to identical current steps were recorded in the same cell, before and after optogenetic stimulation of dopaminergic neurons (black and red traces). Red and gray traces in the OFF state (right) indicate current injections matching or exceeding those shown in the ON state, respectively (left). **b,c**, Time courses of changes in input resistance (R_m) and membrane time constant (τ_m) of dFB neurons during optogenetic stimulation of dopaminergic neurons ($n=7$ cells). Data are means \pm s.e.m. One-way repeated-measures ANOVA detected significant effects of time ($P=0.0135$ for R_m ; $P=0.0222$ for τ_m).



Extended Data Figure 5. Membrane properties of dFB neurons in the ON state. **a**, Input resistances (R_m) of the indicated numbers of cells. Data are means \pm s.e.m. Kruskal-Wallis test failed to detect a significant difference between groups ($P=0.8997$). **b**, Membrane time constants (τ_m) of the indicated numbers of cells. Data are means \pm s.e.m. Kruskal-Wallis test failed to detect a significant difference between groups ($P=0.1682$).



Extended Data Figure 6. Measurements of potassium currents in voltage clamp. **a**, Voltage steps from a holding potential of -110 mV (top) elicited the full complement of potassium currents expressed by a dFB neuron (I_{total} , bottom). **b**, Stepping the same neuron from a holding potential of -30 mV (top) elicited potassium currents lacking the A-type component ($I_{\text{non-A}}$, bottom). **c**, Digital subtraction of $I_{\text{non-A}}$ (**b**, bottom) from I_{total} (**a**, bottom) yielded an estimate of I_A . Note the expanded timescale. **d**, Individual (gray) and average (black) A-type currents of 7 dFB neurons, evoked by step depolarization to 40 mV. The magenta line represents a single-exponential fit to the average.



Extended Data Figure 7. Loss of Shaker and its interacting partners, Hyperkinetic and Sleepless, from dFB neurons has similar effects on sleep. Sleep in flies expressing *R23E10-GAL4* driven RNAi targeting Shaker, Hyperkinetic, or Sleepless and parental controls (circles denote individual flies; horizontal lines indicate group means). One-way ANOVA detected a significant genotype effect ($P < 0.0001$); green colour indicates significant differences from both parental controls in pairwise post-hoc comparisons.